Available online at www.sciencedirect.com
SCIENCE DIRECT
Journal of Catalysis 230 (2005) 249–253
JOURNAL OF CATALYSIS
www.elsevier.com/locate/jcat

Research Note

# Nanocrystalline $LaCoO_3$ perovskite particles confined in SBA-15 silica as a new efficient catalyst for hydrocarbon oxidation

Nan Yi, Yong Cao *, Yang Su, Wei-Lin Dai, He-Yong He, Kang-Nian Fan *

*Department of Chemistry & Shanghai Key Laboratory of Molecular Catalysis and Innovative Materials, Fudan University, Shanghai 200433, P.R. China*

Received 20 September 2004; revised 29 November 2004; accepted 29 November 2004

Available online 23 December 2004

**Abstract**

Highly crystalline $LaCoO_3$ perovskite particles were prepared by a novel microwave-assisted process with a La–Co citrate complex precursor in the host pores of mesoporous SBA-15 silica. The resulting material exhibited considerably higher catalytic activity in the complete methane oxidation than a $LaCoO_3$/SBA-15 sample prepared by a conventional method with a bulk $LaCoO_3$ perovskite. This suggests that a higher density of lattice defects achieved on the high-surface-area $LaCoO_3$ nanocrystals synthesized by microwave processing is essential for the superior performance of the catalyst.


*Keywords:* $LaCoO_3$ perovskites; Siliceous mesoporous SBA-15; Microwave-assisted processing (MAP); Lattice defects; Methane combustion

## 1. Introduction

Catalytic combustion of methane is an attractive, viable technology for the environmentally friendly production of energy because energy use is more efficient and pollutant emissions are minimal compared with conventional flame combustion [1–4]. Catalyst systems based on supported noble metals have been extensively investigated for the complete oxidation of methane [1–3], but they generally deactivate rapidly under reaction conditions because of sintering and loss of active species. In the development of more suitable catalysts for the combustion of methane, the perovskite-type oxides (PTOs) containing transition-metal ions (e.g., Co, Mn, Fe) have attracted considerable attention recently as promising new hydrocarbon combustion materials because of their high thermal stability and relatively low cost compared with their conventional noble-metal counterparts [5–9]. However, the potential applications of these materials are greatly limited by their small surface areas (generally below 50 $m^2\,g^{-1}$) [7–9].

One possible way of circumventing this problem is to disperse perovskites on porous supports with a high specific surface area to optimize the catalytic performance [10–16]. Recently, silica-based mesoporous materials have been reported to be promising supports for a number of catalytically active species because of their high surface area and stable well-ordered pore structures [17–20]. Here, for the first time, we have found that highly crystalline $LaCoO_3$ perovskites in SBA-15 channels, which are fully accessible to the reaction molecules, can be prepared by novel microwave-assisted processing (MAP) of a La–Co citrate complex precursor inside the SBA-15 host and are highly efficient catalysts for methane combustion. It was demonstrated that the use of microwave heating in the synthesis of dispersed $LaCoO_3$ perovskites makes possible the convenient and rapid generation of SBA-15-hosted perovskite nanocrystals with favorable microstructural modification, resulting in the creation of a high density of lattice defects. This in turn leads to the significant enhancement of their performance for catalytic methane combustion.

* Corresponding authors. Fax: +86 21 65642978.
*E-mail addresses:* yongcao@fudan.edu.cn (Y. Cao), knfan@fudan.edu.cn (K.-N. Fan).

0021-9517/$ – see front matter 
doi:10.1016/j.jcat.2004.11.042

## 2. Experimental

### 2.1. Catalyst preparation

Pure siliceous SBA-15 was prepared according to a procedure in the literature [17]. Conventional and microwave-synthesized $LaCoO_3$ perovskites in SBA-15 hosts were prepared in two steps under similar conditions. Typically, 2.0 g of SBA-15 was impregnated by incipient wetness with an alcoholic solution containing equimolar amounts of La and Co citrate complex precursors (the molar ratio of citric acid to total Co + La cations was fixed at 1), corresponding to 10 wt% $LaCoO_3$ loading, followed by vacuum drying at 60 °C. This process was performed six times to achieve a final $LaCoO_3$ content of 60 wt%. The resulting La–Co citrate complex precursor inside the silica nanotubes was subjected to microwave irradiation in a domestic microwave oven (500 W, 2.45 GHz) for 6 min to obtain the final black powder (MLC-60). During the microwave treatment, the maximum temperature was ca. 700 °C (monitored by an optical pyrometer; Minolta). With a similar procedure, except that the final calcination step was conducted in a muffle oven at 600 °C for 6 h in air, the CLC-60 sample containing the same $LaCoO_3$ content in the SBA-15 host was prepared. For comparison, a reference bulk $LaCoO_3$ sample was prepared by calcination of the La–Co precursors, obtained by a conventional "citrate method" at 700 °C for 4 h in air [21].

### 2.2. Catalyst characterization

X-ray diffraction (XRD) patterns were collected on a Bruker AXS D8 Avance X-ray diffractometer with Cu-$K_\alpha$ radiation ($\lambda = 1.5418$ Å). The BET surface area and the pore volume were determined by $N_2$ physical adsorption at 77 K on a Micromeritics TriStar 3000 adsorption apparatus. The active oxygen sites on the catalysts were studied by temperature-programmed desorption of $O_2$ ($O_2$-TPD) monitored with an on-line quadrupole mass spectrometer (QMS200, Balzers OmniStar). TEM images were recorded digitally with a Gatan slow-scan charge-coupled device (CCD) camera on a JEOL 2011 electron microscope operating at 200 kV.

### 2.3. Catalytic tests

The catalytic oxidation of methane was carried out in a fixed-bed quartz microcatalytic flow reactor (6 mm OD, 4 mm ID) at atmospheric pressure with 100 mg of catalyst (60–80-mesh) loading [19]. To prevent the development of hot spots in the catalytic bed, the catalysts were diluted with 300 mg of quartz powder (40–60-mesh). The feed was a mixture of $CH_4/O_2$/He with a molar ratio of 1:4:95 and a total gas flow of 10–100 mL $min^{-1}$, giving a space velocity (GHSV) in the range of 20,000–200,000 $h^{-1}$. The feed and the product gases were analyzed on-line with a gas chromatograph (Type GC-122, Shanghai).

## 3. Results and discussion

Table 1 gives the characteristics of the two $LaCoO_3$/SBA-15 samples with a high $LaCoO_3$ loading of 60 wt%, prepared by conventional and microwave-assisted methods, and the parent SBA-15 and bulk $LaCoO_3$ perovskite reference samples. The $LaCoO_3$ perovskite phase (XRD) of the bulk $LaCoO_3$ reference sample, prepared by the conventional citrate method, had an average crystal size of 15.4 nm and an extremely low surface area of 6 $m^2\,g^{-1}$ (Table 1). Incorporation of $LaCoO_3$ perovskite into the SBA-15 mesopores results in a shift in the X-ray diffraction peaks to higher angles in the low-angle region, together with a strong attenuation of the peak intensities. According to Wang et al. [20] and Sauer et al. [22], this does not indicate degradation of the SBA-15 structure, but may be a consequence of the X-ray scattering on the confined $LaCoO_3$ nanocrystals and the reduced SBA-15 concentration in the composites. TEM unambiguously confirmed the integrity of the SBA-15 structure in the $LaCoO_3$/SBA-15 composites of sample MLC-60, which further revealed that the darker $LaCoO_3$ particles (as verified by EDX) were uniformly dispersed in the SBA-15 nanotubular

Table 1
Characteristics of $LaCoO_3$ perovskites in SBA-15 hosts

| Sample | $S_{BET}$[a] ($m^2\,g_{cat}^{-1}$) | $NS_{BET}$[b] ($m^2\,g_{SiO_2}^{-1}$) | PV ($cm^3\,g^{-1}$) | PD (nm) | $d_{XRD}$[c] (nm) | Cell parameters (Å)[d] | |
|---|---|---|---|---|---|---|---|
| | | | | | | *a* | *c* |
| SBA-15 | 695 | 695 | 1.22 | 7.6 | / | / | / |
| MLC-60 | 204 (84) | 510 | 0.44 | 6.0 | 6.5 | 5.411 | 13.263 |
| CLC-60 | 185 (76) | 463 | 0.36 | 5.3 | 7.2 | 5.413 | 13.222 |
| $LaCoO_3$ | 6 | / | 0.04 | / | 15.4 | 5.438 | 13.096 |
| $LaCoO_3$[e] | / | / | / | / | / | 5.441 | 13.088 |

[a] The data in parentheses are the surface area of the $LaCoO_3$ particles estimated by $SA = 6000X/(\rho d)$, where $\rho = 6.5644\ g\,cm^{-3}$ (theoretical density of $LaCoO_3$ perovskite), $d$ = particle diameter, $X$ = loading.
[b] The specific surface area ($NS_{BET}$) normalized to 1 g of the host material.
[c] The average particle diameters calculated from XRD data based on Sherrer equation.
[d] The lattice parameters calculated by the square method according to the Cohen procedure [23].
[e] Standard data from Powder Diffraction File 25-1060 [24].

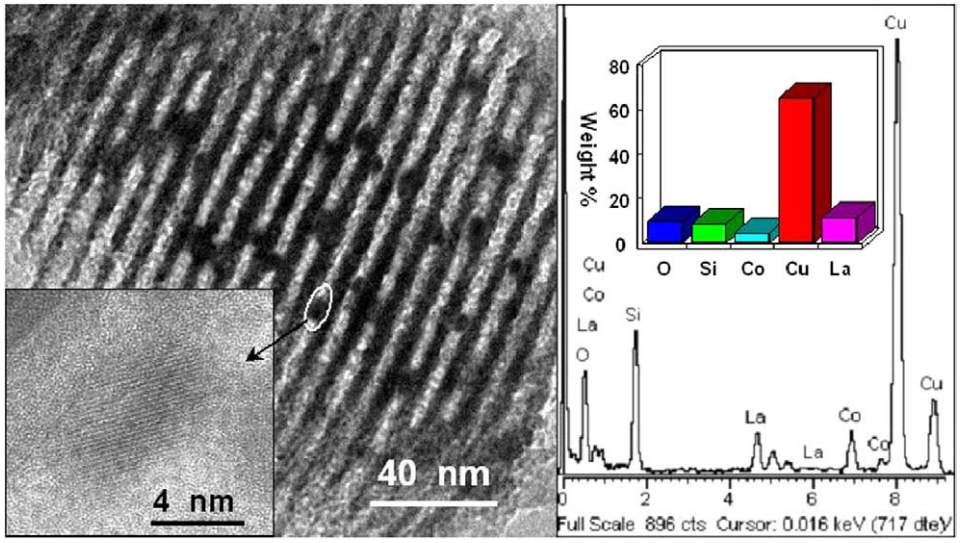


Fig. 1. TEM micrographs (left, inset shows image of the encircled area at higher magnification) and corresponding EDX spectrum (right) of sample MLC-60.

channels (Fig. 1). The parallel fringes across the nanocrystal images had a periodicity of 2.65 Å ($LaCoO_3$) (inset in Fig. 1), which corresponds to planes with a $d$-spacing of $d_{110} = \tilde{2}719$ Å in the $LaCoO_3$ perovskite structures [23]. The average particle size of the $LaCoO_3$ particles in the MLC-60 sample is 5–8.5 nm, in good agreement with the value calculated from the peak broadening of the X-ray diffraction pattern (Table 1).

The preservation of the well-defined hexagonal arrangement of the SBA-15 framework, after the introduction of $LaCoO_3$ perovskite, is further supported by the $N_2$ adsorption data. The specific surface area and the cumulative pore volume of the parent SBA-15 were 695 $m^2\,g^{-1}$ and 1.22 $cm^3\,g^{-1}$, respectively. The results in Table 1 clearly demonstrate that the insertion of $LaCoO_3$ perovskite causes a remarkable loss of pore volume and a reduction in the pore diameter of the SBA-15 host materials. However, the decrease in specific surface area in the $LaCoO_3$-loaded samples is due mainly to an increase in the density of the materials upon La–Co oxide incorporation. This is reflected by the high values of the specific surface areas normalized to 1 g of the host material (Table 1). The pore volume and pore diameter of the MLC-60 sample are much higher than those of the CLC-60 sample prepared by the conventional method, demonstrating the potential of the microwave technique for preparing dispersed perovskite catalysts with favorable textural properties. Moreover, a pronounced modification of the lattice parameters of the MLC-60 sample with respect to the conventional sample is observed [23,24], which further illustrates the unusual dielectric heating effect of microwave irradiation on the microstructure of the $LaCoO_3$ perovskite lattice.

Fig. 2 presents the methane conversion as a function of temperature over MLC-60, CLC-60, and the bulk $LaCoO_3$ perovskite catalysts. The light-off temperatures ($T_{10}$, defined as 10% conversion of methane) were at 406, 477, and

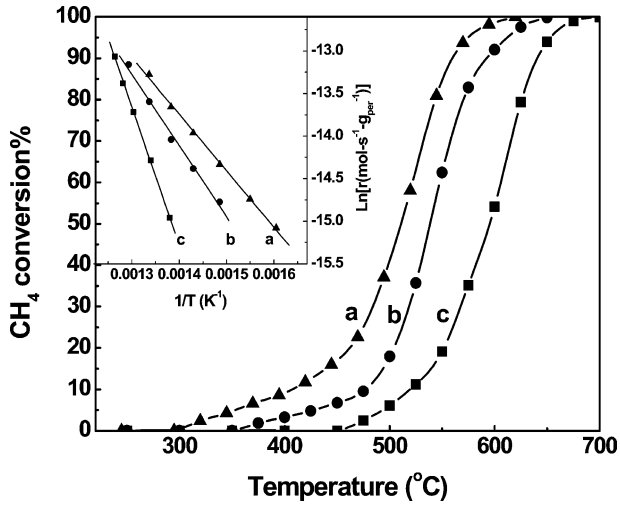


Fig. 2. Light-off curves of methane conversion as a function of temperature measured with (a) MLC-60, (b) CLC-60, and (c) bulk $LaCoO_3$ perovskites. Inset shows the corresponding Arrhenius plot.

521 °C, and the half-conversion temperatures ($T_{50}$) were at 510, 538, and 596 °C for MLC-60, CLC-60, and the bulk $LaCoO_3$ perovskite samples, respectively. Moreover, the apparent activation energy of the MLC-60 sample for methane combustion was estimated to be $\sim 54$ $kJ\,mol^{-1}$ (inset in Fig. 2), in sharp contrast to the much higher values of 142 and 68 $kJ\,mol^{-1}$ for the bulk $LaCoO_3$ perovskite and the conventionally prepared CLC-60 sample, respectively. This clearly indicates the considerably higher catalytic activity of the MLC-60 sample prepared in the microwave than that of the reference samples. The MLC-60 catalyst attained full $CH_4$ conversion by 620 °C; no hysteresis was observed in catalyst performance during heating–cooling–restarting cycles. We believe that the excellent low-temperature catalytic activity of this system arises in part from the unusual microstructure of the MLC-60 sample.

The "low-temperature step," observed with the $LaCoO_3$ perovskite supported on MCM-41 and previously reported by Nguyen et al. [16], is not obtained with MLC-60 or CLC-60. This "step" is suggested to be associated with the occurrence of internal diffusion in the long, regular cylindrical pores of the mesoporous MCM-41 support [16]. The fact that such limitations are not observed with the present SBA-15-supported $LaCoO_3$ perovskites is probably due to the ultra-large pore diameter of this material, which results in much less limitation of diffusion. On the other hand, the "normalized activity" (based on the surface area of the crystalline $LaCoO_3$ perovskite phase) (Table 1) of the present SBA-15-supported $LaCoO_3$ perovskites appears to be lower than that of the bulk perovskite sample, possibly because of the interactions of the $LaCoO_3$ particles with the SBA-15 support or deviations from a spherical morphology.

$O_2$-TPD has been carried out to clarify the nature of the surface oxygen species involved in the SBA-15-loaded $LaCoO_3$ samples for catalytic methane oxidation (not shown). The MLC-60 sample shows two peaks: the $\alpha$-peak (desorbed below 650 °C), ascribed to superficial oxygen species weakly bound to the surface, and the $\beta$-peak, associated with lattice oxygen originating from the bulk of the samples [9,25]. It is revealed that the amount of oxygen released from MLC-60 is much higher than that of bulk $LaCoO_3$ perovskite and the conventionally prepared CLC-60 sample. This confirms the presence of a higher density of lattice defects and a higher specific surface area of MLC-60 than of bulk $LaCoO_3$ perovskite, which may be the main reasons for the markedly enhanced $CH_4$ combustion activity. However, the superficial $\alpha$-oxygen species may also contribute to some extent to the superior performance of the present MLC-60 sample.

Microwave-assisted catalyst synthesis has attracted much attention because it is a much faster, simpler, and more energy-efficient technique for synthesizing new catalytic materials with improved microstructures compared with conventional methods [26–28]. The currently available methods for the synthesis of perovskite oxides generally require high temperatures, tedious multistep processing, and long preparation times [26]. By combining microwave heating with mixed metal nitrates, which absorb microwaves easily, Jayaram et al. [28] demonstrated the possibility of using microwave processing to synthesize the perovskite oxides of $LaMO_3$ (M = Mn, Fe, Cr, Co, Al) with excellent catalytic activity for the reduction of aromatic nitro compounds with propan-2-ol. For the first time, we have demonstrated the advantage of microwave-assisted processing as a promising new synthetic method for the rapid and convenient generation of $LaCoO_3$ perovskite nanocrystals in SBA-15 hosts with favorable microstructural modification, which exhibit superior catalytic performance in the complete combustion of methane. Preparation with microwave-assisted processing takes much less time than conventional muffle-oven heating, making it an attractive alternative for practical applications.

## 4. Conclusions

Microwave-assisted processing of La–Co citrate complex precursors inside the nanotubular pores of mesostructured SBA-15 silica allows the incorporation of up to 60 wt% $LaCoO_3$ perovskites, as 5–8.5-nm nanocrystals, into the mesopores. The $LaCoO_3$ nanocrystals are uniformly distributed along nanotubes of mesostructured silica hosts without pore blockage. The superior performance of the confined $LaCoO_3$ nanocrystals in the complete oxidation of methane has been attributed to their high surface area and a much higher density of lattice defects on the microwave-derived samples.

## Acknowledgments

This work was supported by the National Science Foundation of China (grants 20473021 and 20203003), the National Major Basic Research Program of China (grant 2003CB615807), and the Committee of Shanghai Science and Technology (grant 02QA14006).

## References

[1] A.J. Zarur, J.Y. Ying, Nature 403 (2000) 65.
[2] M.D. Fokema, J.Y. Ying, Catal. Rev. Sci. Eng. 43 (2001) 1.
[3] J. Chaouki, C. Guy, C. Sapundzhiev, D. Kusohoesky, D. Klvana, Ind. Eng. Chem. Res. 33 (1994) 2957.
[4] K. Sekizawa, K. Eguchi, H. Widjaja, M. Machida, H. Arai, Catal. Today 28 (1996) 245.
[5] M.A. Peña, J.L.G. Fierro, Chem. Rev. 101 (2001) 1981.
[6] L.G. Tejuca, J.L.G. Fierro (Eds.), Properties and Application of Perovskite-Type Oxides, Marcel Dekker Inc., New York, 1992.
[7] S. Kaliaguine, A. Van Neste, V. Szabo, J.E. Gallot, M. Bassir, R. Muzychuk, Appl. Catal. A 209 (2001) 345.
[8] S. Cimino, R. Pirone, L. Lisi, M. Turco, G. Russo, Catal. Today 59 (2000) 19.
[9] V. Szabo, M. Bassir, A. Van Neste, S. Kaliaguine, Appl. Catal. B 42 (2003) 265.
[10] N. Mizuno, H. Fujii, H. Igarashi, M. Misono, J. Am. Chem. Soc. 114 (1992) 7151.
[11] S.D. Peter, E. Garbowski, V. Perrichon, M. Primet, Catal. Lett. 70 (2000) 27.
[12] S. Cimino, S. Colonna, S. De Rossi, M. Faticanti, L. Lisi, I. Pettiti, P. Porta, J. Catal. 205 (2002) 309.
[13] C.T. Kresge, M.E. Leonowicz, W.J. Roth, J.C. Vartuli, J.S. Beck, Nature 359 (1992) 710.
[14] D. Trong On, D. Desplantier-Giscard, C. Danumah, S. Kaliaguine, Appl. Catal. A 222 (2001) 299.
[15] A. Wigen, N. Anastasivic, A. Hollnagel, D. Werner, F. Schüth, J. Catal. 193 (2000) 248.
[16] S.V. Nguyen, V. Szabo, D. Trong On, S. Kaliaguine, Micropor. Mesopor. Mater. 54 (2002) 51.
[17] D.Y. Zhao, J.L. Feng, Q.S. Huo, N. Melosh, G.H. Fredrickson, B.F. Chmelka, G.D. Stucky, Science 279 (1998) 548.
[18] M.V. Landau, L. Titelman, L. Vradman, P. Wilson, Chem. Commun. (2003) 594.

[19] Y.M. Liu, Y. Cao, N. Yi, W.L. Feng, W.L. Dai, R.S. Yan, H.Y. He, K.N. Fan, J. Catal. 224 (2004) 417.
[20] X. Wang, M.V. Landau, H. Rotter, L. Vradman, A. Wolfson, A. Erenberg, J. Catal. 222 (2004) 565.
[21] M.S.G. Baythoun, F.R. Sale, J. Mater. Sci. 17 (1982) 2757.
[22] J. Sauer, F. Marlow, F. Schüth, Phys. Chem. Chem. Phys. 3 (2001) 3679.
[23] H.P. Klug, L.E. Alexander, X-Ray Diffraction Procedures, Wiley, New York, 1954.
[24] Powder Diffraction Files, JCPDS, International Center for Diffraction Data, 1984.
[25] M. Iwamoto, Y. Yoda, N. Yamazoe, T. Seiyama, J. Phys. Chem. 72 (1982) 2564.
[26] K.J. Rao, B. Vaidhyanathan, M. Ganguli, P.A. Ramakrishinan, Chem. Mater. 11 (1999) 882.
[27] T.A. Nissinen, Y. Kiros, M. Gasik, M. Leskelä, Chem. Mater. 15 (2003) 4974.
[28] A.S. Kulkarni, R.V. Jayaram, Appl. Catal. A 252 (2003) 225.